Determination of Instantaneous Powers from a Novel Time-Domain Parameter Identification Method of Non-Linear Single-Phase Circuits

Francisco G. Montoya, Francisco de León, *Fellow, IEEE*, Francisco Arrabal-Campos, and Alfredo Alcayde

***Abstract*—This paper proposes a systematic method for the identification of the load circuit parameters (say the R, L, and C elements) based only on the information of the instantaneous voltage and current measured at the point of common coupling (pcc). Geometric Algebra (GA) and concepts of differential geometry are used to produce a rigorous mathematical framework. The identification is formulated as a multidimensional geometrical problem that is solved conveniently by means of GA. Once the passive elements of the load have been identified, the active and reactive powers can be computed from first electromagnetic principles (Maxwell Equations). The theory is general and is verified with linear and nonlinear circuits. The paper shows single-phase circuits but the theory can be extended to three-phase circuits. The method is easy to program and has shown to be very robust for all tested cases. Because of its generality, the method presented will find applications beyond electric circuits.**

***Index Terms*—Circuit parameter identification, geometric algebra, nonlinear circuits, power definitions.**

I. Introduction

POWER exchanges between a source and non-linear and/or unbalanced loads have been the subject of much research for over 100 years. Electric power concepts can be traced back to the work by Joule in 1841 [1]. Joule uncovered experimentally that electric power was proportional to the product of voltage and current ($P \propto VI$) for dc circuits. At that time, a system of units did not yet exist and an equality sign could not be established. In 1873, Maxwell wrote his 20 equations in the cgs measurement system [2]. Heaviside reduced these 20 equations to today's four Maxwell Equations in 1881. Poynting published the theorem of conservation of electromagnetic energy in 1884 [3].

The next set of important contributions towards a power theory for ac circuits were done by Kennelly and Steinmetz between the years of 1893 and 1900. Kennelly proposed the use of complex numbers for the analysis of ac electric circuits in [4]. In particular, Kennelly used complex numbers to describe Ohm's law and coined the word "impedance". Steinmetz included Kirchhoff laws a few months later [5]. In 1900, Steinmetz published the power theory that is still in use today for linear systems ($S = P + jQ = VI^*$), which he called the "double frequency product" [6]. He also defined "power" (today's active power) and "wattless power" (our reactive power). However, as early as 1920 , problems with Steinmetz powers for unbalanced circuits were identified in a series of discussion papers that span 70 pages [7]. In 1933 in another series of papers (covering 60 pages) several inconsistencies with the definition of reactive power for nonlinear circuits were discussed [8].

Over the next close to 80 years since, there have been a large number of authors proposing and challenging power theories. A few of the most important names (with sincere apologies to those we missed) in alphabetic order include: Akagi, Aredes, Budeanu, Cohen, Czarnecki, Depenbrock, Emanuel, Ferrero, Filipski, Fryze, Gaunt, Ghassemi, Kusters, Lev-Ari, Malengret, Menti, Moore, Nabae, Peng, Salmerón, Shepherd, Sutherland, Watanabe, Willems, and Zand.

Even after the IEEE published Standard 1459-2010, there is no agreement in the community about what the physical correct powers are (or are supposed to be). The standard itself recognizes this fact [9]. Just in the last decade (after the publication of the standard) we can cite many papers proposing new definitions or interpretations [10]–[14]. Three books have been written on the subject [15]–[17]. A fourth book will be available later in 2021 [18]. The available preview of [18] contains over one thousand references. Attempts have been made to represent power phenomena in electric circuits directly in the time domain. For example, [19] presents the Consevative Power Theory (CPT), which uses effectively the concept of homo-variables. Unfortunately, however, the instantaneous powers computed result in powers that are not consistent with Maxwell equations.

This paper provides a new mathematical framework based on Geometric Algebra (GA) and Differential Geometry (DG) to solve the problem of system parameter identification introduced in [20]. Space trajectories described by time variant space vectors (called spacors in this paper) for single-phase circuits are presented. The new formulation is completely general and applicable to continuous and discrete signals. Because of its generality, the new method is applicable to three- or n-phase systems by adding more dimensions.

Geometric algebra is a promising and powerful mathematical framework, ideal to perform calculations with 1-dimensional (vectors) or n-dimensional objects [21]. It is generally applicable to a wide range of engineering problems and gives greater physical insight than the algebra of complex numbers commonly used today to solve electric circuits [22]. GA is currently used in many fields of physics and engineering including: quantum mechanics [23], electromagnetics [24], relativity [23], robotics [25], and others. Unfortunately, it has not been widely adopted in electrical power engineering where complex numbers and frequency domain calculations have been favored. However, its usefulness has been recently proved in [22] and [26], [27] for both time and frequency domains. As shown below, GA brings a new dimension to the solution of nonlinear circuits. It allows for the determination of the power

F. G. Montoya, F. M. Arrabal-Campos and A. Alcayde are with the Department of Engineering at University of Almeria. La Cañada de San Urbano, 04120 Almeria, Spain (Email: pagilm@ual.es).

F. de León is with the Department of Electrical and Computer Engineering at New York University. Five Metrotech Center, Brooklyn, NY 11201, USA (Email: fdeleon@nyu.edu).

This work was supported in part by Ministry of Science and Innovation under Grant PGC2018-098813-B-C33

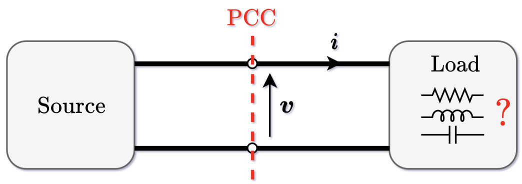

Figure 1. Pictorial representation of the problem solved in this paper. v and i are the instantaneous voltage and current measured at the point of common coupling (pcc).

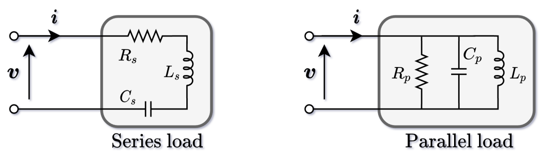

Figure 2. Equivalent circuits for the representation of the load. All variables and parameters are functions of time; left) series equivalent; right) parallel equivalent.

consumed in nonlinear resistors and the oscillatory energy in non linear inductors directly from the terminal voltage and current.

The method proposed in this paper is easy to implement, gives accurate results, and provides great flexibility in the selection of the model topology. Different circuit models can be synthesized when particular conditions are to be highlighted. In this paper, a number of examples covering linear and nonlinear circuits with sinusoidal and non-sinusoidal excitations, demonstrate the robustness of the new method.

Application examples on electric circuit parameter identification at the point of common coupling (pcc) are presented. However, the techniques put forward in this paper have applications beyond the parameter identification of electric circuits. For example, current compensation through active and passive filters can be performed in a straightforward way. NonIntrusive Load Monitoring (NILM) is another important field where the proposed technique can be applied. Other fields such as power line fault detection and transformer parametrization can benefit from the techniques of this paper. The method can even be applied to other fields of engineering, for example, to mechanical systems through the electromechanical analogy [28]. The method can be used to obtain the mass, spring, and damping parameters.

II. Theoretical Background

A. Problem Statement

The problem that this paper solves is the identification of the load circuit parameters (R, L, C) from only the knowledge of the instantaneous voltage v and current i measured at the point of common coupling (pcc). Fig. 1 depicts the problem that we undertake. It has been shown in [20] that all the information necessary to characterize a load is contained in the terminal voltage and current signals. Fig. 2 shows two possible equivalent circuits: series and parallel. According to the IEEE Standard 100 ("The Authoritative Dictionary of IEEE Standards Terms") [29] page 390: "(an) equivalent circuit is an arrangement of circuit elements that has characteristics, over a range of interest, electrically equivalent to those of a different circuit or device." Our interpretation of this definition is that an equivalent circuit is a theoretical circuit that retains all of the electrical characteristics of the circuit it represents (in our case instantaneous current, power, and energy). The unknown circuit parameters R, L and C vary with time and accurately describe the energy exchanges between the source and the load. Several circuit topologies can be synthesized, but here we discuss only the two simplest ones.

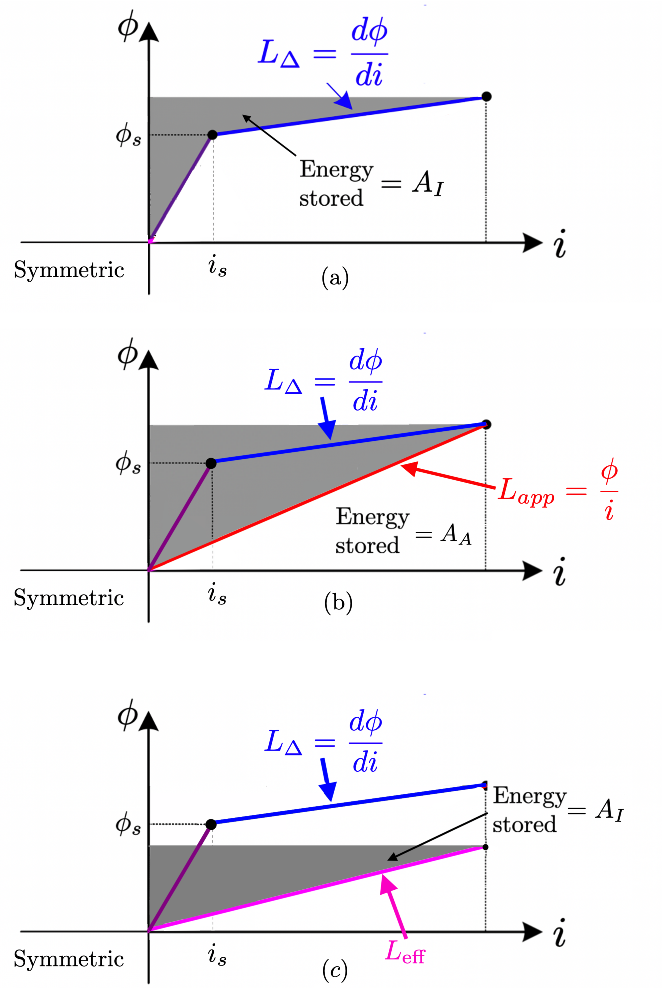

Figure 3. Illustration of the apparent, incremental, and effective inductances for a linear piece-wise variation. In the linear region $-\phi_s \leq \phi \leq \phi_s$ all inductances are the same.

B. Assumptions

It is supposed that the variation with time of the circuit parameters takes place in steps. In other words, all nonlinearities are transformed into time-varying functions since all functions (linear or nonlinear) can be described using time as the independent variable. Consequently, parameters R, L, and C are assumed to be constant for a given period of time (larger than the sampling rate). For continuous variations, an analytic formulation can still be derived based on differential geometry. This is not necessary at present because all modern instrumentation is digital.

We remark that the parameter identification is done point-by-point. Therefore, non-linear variations in the circuit parameters are incremental in nature. For a nonlinear inductor, one needs to distinguish between apparent inductance, incremental inductance, and effective inductance. Fig. 3 illustrates the three concepts for a linear piece-wise representation of a saturating inductor. Fig. 3(a) shows the incremental inductance and its energy stored. We see that the inductor is unsaturated from 0 to ϕ_s. At ϕ_s the incremental inductance reduces (smaller slope). The energy stored in nonlinear inductors is computed according to Maxwell equations as:

$$w_{\text{stor}(L)} = \frac{1}{2}\iint_V \bar{H}\cdot d\bar{B} \longrightarrow w_{\text{stor}(L)} = \int i d\phi \qquad (1)$$

The area described by (1) is shown in Fig. 3(a) as the shaded region labeled A_I. The incremental inductance properly relates current with flux and also gives the correct energy stored. The apparent inductance is a linear inductance that relates flux with current correctly. Fig. 3(b) shows the apparent inductance for the last point of the curve. This inductance can be used for steady state (frequency domain) calculations as current and flux follow the nonlinear curve. However, this inductance cannot be used to compute the energy stored. With (1) one computes the energy stored of this inductance as area A_A. One can see from Fig. 3(b) that $A_A > A_I$. The apparent inductance is useful in circuit theory when the objective is to compute voltages and current using linear inductors to represent the global behavior of a circuit with non-linear inductors. However, one should be aware that the energy stored from the apparent inductance is not correct. Fig 3(c) illustrates the effective inductance. This is the inductance of a linear inductor with the same stored energy (A_I) than the incremental inductor (see the shaded region in Fig. 3(c)). However, this inductor cannot be used to compute the relationship between flux and current; see more on this in Section VI.

Throughout the paper we use inductance L and its inverse, Γ to represent incremental values L_Δ and Γ_Δ. Apparent and effective inductances are explicitly labeled L_{app} and L_{eff} Note that resistors and capacitors in a power system load are normally linear. They can be switched on and off mechanically or electronically. However, non-linear models can be organically introduced in the formulation. Under the above assumptions, one can write Kirchhoff Voltage Law (KVL) for the series circuit (Fig. 2 left) as:

$$v(t) = R_\Delta i(t) + L_\Delta \frac{d}{dt} i(t) + \frac{1}{C_\Delta}\int i(t) \qquad (2)$$

which is written in short as follows:

$$v = Ri + Li' + S\tilde{i} \qquad (3)$$

where i' is the time derivative of the current i, $\tilde{i}$ stands for the integral of i, and $S = 1/C$ is the elastance (inverse of the capacitance). Kirchhoff Current Law (KCL) can be applied to the parallel circuit (Fig. 2 right) as follows:

$$i(t) = G_\Delta v(t) + \Gamma_\Delta \int v(t) + C_\Delta \frac{d}{dt} v(t) \qquad (4)$$

which is written in short for convenience as:

$$i = Gv + \Gamma\tilde{v} + Cv' \qquad (5)$$

As before v' is the time derivative of the voltage v, $\tilde{v}$ stands for the integral of v, $G = 1/R$ is the conductance, and $\Gamma = 1/L$ is the inverse of the inductance. Γ is called *compliance* in this paper because of its resemblance with mechanical systems that use this concept as the reciprocal of stiffness to measure flexibility.

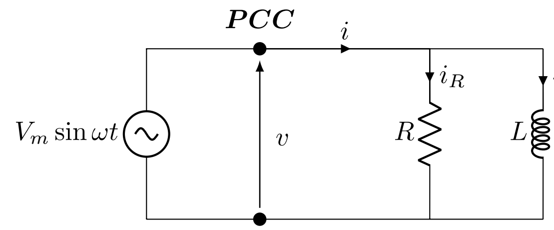

Figure 4. Linear RL parallel circuit with sinusoidal excitation used to illustrate the application of the method.

C. Problem Formulation using Geometric Algebra and Differential Geometry

In this section, the calculation of the circuit parameters is done using very basic concepts of Geometric Algebra (GA). Appendix A gives a detailed description of the operations and rules used here. The fundamental operation used to derive the framework is the wedge product from exterior algebra [30]. This product allows constructing new geometric elements known as k-vectors. The process starts from a very simple axiomatic property for vectors, i.e.,

$$\boldsymbol{a}\wedge\boldsymbol{a} = 0 \qquad (6)$$

which means that the wedge product of a vector $\boldsymbol{a}$ by itself is zero. The wedge product of two different vectors builds up a new object known as bivector (2-vector). Interestingly enough, this bivector represents a plane with direction, sense, and magnitude (see Appendix A). Note that the span of two vectors (widely used in linear algebra) is different from a bivector. The former refers to all linear combinations of the generating vectors (which is a new vector), while the latter is a 2-dimensional geometric object. The wedge product can be extended to more dimensions seamlessly. For example, for a vector space of 3 dimensions, the wedge product of three different vectors gives a trivector (3-vector), i.e., a volume object.

Apart from exterior and geometric algebra, concepts of Differential Geometry (DG) are also needed. We use vectors that describe curves in n-dimensional Euclidean spaces. These curves can be analyzed in terms of the mathematical concept of invariants, for example, curvature, torsion, etc. The most useful concept is the osculating plane (2D) or osculating volume (3D) [31]. These are local tangent spaces to the curve at every point. They allow for the analytical identification of the RLC parameters. See Appendix B for more details.

The identification process includes the following steps: (a) define an appropriate vector with an adequate number of dimensions and suitable coordinates (always voltage or current variables, along with derivatives and/or integrals). To start, the vector must include voltage and current (so far two dimensions). Additional dimensions are needed depending of the number of elements that the sought circuit will have. For a circuit with two elements, series or parallel, we add one dimension. For a circuit with three elements, we need to add two dimensions. The additional variables are selected in a way that when we apply KVL (for a series circuit) or KCL (for a parallel circuit) the variables can be combined. Thus for an inductive series element we include the derivative of the current ($v = Li'$). For an inductive parallel circuit we include the integral of the voltage ($i = \Gamma\tilde{v}$). This vector defines a curve in space because of the time dependency. We call these special vectors *spacors* (acronym of "space vectors"). They must be selected judiciously depending on the desired circuit model topology (see Section III); (b) apply KVL and/or KCL to find linear combinations among the variables; (c) create a new dimensionally reduced frame and find the tangent (osculating) space to the curve using GA and DG; (d) compare one-to-one the terms of the resulting plane (or volume) and the osculating plane (or volume) to visualize the analytical equations that yield the circuit parameters.

III. Derivation of the Parallel Equivalent Circuit

A convenient way to understand the application of GA to system identification is to start with a simple parallel RL circuit with constant parameters and sinusoidal excitation as shown in Fig. 4. This requires of the calculation of only two parameters R and L. To avoid singularities, when the current is zero for longer that a zero crossing, it is better to compute the reciprocals G and Γ

To compute the parallel circuit we follow the method described in the previous section. Let us start by defining a vector (*spacor*) that contains voltage, voltage integral, and current. This selection is made for mathematical convenience looking at combining the variables in (5). The key idea for building the spacor is to chose as coordinates those components of the voltage (including derivatives and integrals) that are already present in (5) by means of KCL. The last coordinate of the spacor should be the current. Following this reasoning, the selected threedimensional spacor is:

$$\boldsymbol{y} = v\boldsymbol{e}_1 + \tilde{v}\boldsymbol{e}_2 + i\boldsymbol{e}_3 \tag{7}$$

where $\boldsymbol{e}_1$, $\boldsymbol{e}_2$ and $\boldsymbol{e}_3$ form the orthonormal vector basis that spans the Euclidean 3D space. Substituting KCL (5) (without C) in (7) we get:

$$\boldsymbol{y} = v\boldsymbol{e}_1 + \tilde{v}\boldsymbol{e}_2 + (Gv + \Gamma\tilde{v})\boldsymbol{e}_3 \tag{8}$$

Note that the above spacor $\boldsymbol{y}$ is a function of voltage and voltage integral only. Collecting terms in (8) we get:

$$\boldsymbol{y} = v\underbrace{(\boldsymbol{e}_1 + G\boldsymbol{e}_3)}_{\boldsymbol{a}} + \tilde{v}\underbrace{(\boldsymbol{e}_2 + \Gamma\boldsymbol{e}_3)}_{\boldsymbol{b}} \tag{9}$$

It can be shown that vectors $\boldsymbol{a}$ and $\boldsymbol{b}$ are linearly independent (although not orthogonal) so they span a 2D subspace; see Appendix A. Therefore, the curve or trajectory defined by vector $\boldsymbol{y}$ is contained in a plane that can be conveniently computed from the wedge product of vectors $\boldsymbol{a}$ and $\boldsymbol{b}$ as follows:

$$\boldsymbol{K} = \boldsymbol{a} \wedge \boldsymbol{b} = (\boldsymbol{e}_1 + G\boldsymbol{e}_3) \wedge (\boldsymbol{e}_2 + \Gamma\boldsymbol{e}_3) \tag{10}$$

From elementary GA operations, the above equation can be written as:

$$\boldsymbol{K} = \boldsymbol{e}_{12} - G\boldsymbol{e}_{23} - \Gamma\boldsymbol{e}_{31} \tag{11}$$

Now we use the concept of osculating plane in differential geometry to compute the tangent plane to the curve using the measurements at the pcc. For this, we take the first and second derivatives of vector $\boldsymbol{y}$ resulting in

$$\boldsymbol{y}' = v'\boldsymbol{e}_1 + v\boldsymbol{e}_2 + i'\boldsymbol{e}_3 \tag{12}$$
$$\boldsymbol{y}'' = v''\boldsymbol{e}_1 + v'\boldsymbol{e}_2 + i''\boldsymbol{e}_3 \tag{13}$$

In geometric algebra, a plane can be computed directly from the wedge product of two vectors [30]. In this case, the osculating plane defined by $\boldsymbol{y}'$ and $\boldsymbol{y}''$ is:

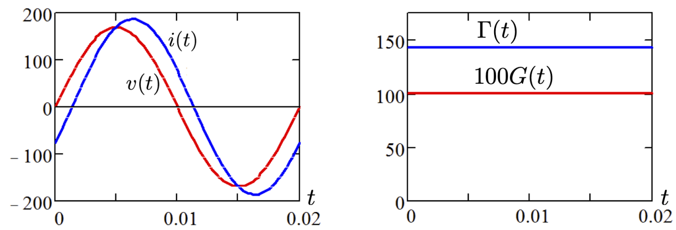

Figure 5. Time variation of parameters for the case of Fig. 4. left) voltage and current vs time at the pcc; right) identified conductance G and compliance Γ.

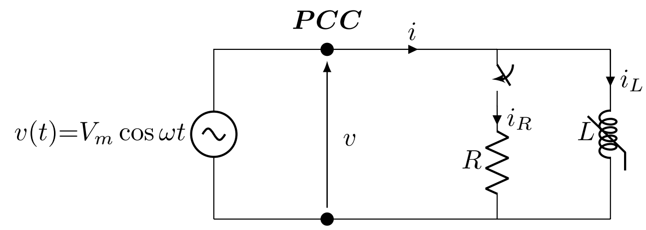

Figure 6. Nonlinear circuit used to illustrate the capabilities of the method to identify circuit parameters

$$\boldsymbol{K}_{\text{osc}} = \boldsymbol{y}' \wedge \boldsymbol{y}'' = \left(v'^2 - vv''\right)\boldsymbol{e}_{12} + \left(vi'' - v'i'\right)\boldsymbol{e}_{23} + \left(v''i' - v'i''\right)\boldsymbol{e}_{31} \tag{14}$$

Both planes $\boldsymbol{K}$ and $\boldsymbol{K}_{osc}$ are two-dimensional subspaces (that live in a 3D space) with the same direction but possibly different magnitude. Thus, they are scaled versions of each other. This implies that the ratio between any two pair of their coordinates should be the same. Therefore, comparing term-to-term of $\boldsymbol{K}$ in (11) with $\boldsymbol{K}_{osc}$ in (14) we observe that the ratios of the coordinates of bivectors $\boldsymbol{e}_{23}$ and $\boldsymbol{e}_{12}$ give G and bivectors $\boldsymbol{e}_{31}$ and $\boldsymbol{e}_{12}$ give Γ:

$$G = \frac{v'i' - vi''}{v'^2 - vv''} \qquad \Gamma = \frac{v'i'' - v''i'}{v'^2 - vv''} \tag{15}$$

When (15) is evaluated at each point, the equivalent conductance G and compliance Γ at every instant are obtained. Note that no assumptions have been made about the type of excitation or nature of the circuit. Therefore, these equations are completely general and, as shown below, are applicable to linear and nonlinear circuits with sinusoidal and nonsinusoidal excitations. Also note that the Teager-Kaiser (TKEO) energy operator [32] is obtained by our method in the denominator of (14). This TKEO is usually defined as

$$\Psi_c[v(t)] = \left[\frac{dv(t)}{dt}\right]^2 - v(t)\frac{d^2v(t)}{dt^2}$$

It was originally conceived to track energy in time domain signals and is used in power systems for frequency and energy estimation [33].

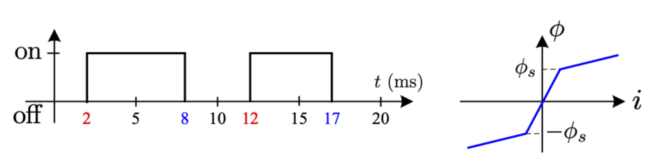

Figure 7. Switching states on/off for circuit in Fig. 6 and nonlinear $\phi - i$ curve.

A. Example 1: Parallel Circuit with Sinusoidal Excitation and Linear $R - L$ Elements

The first example consists in the identification of the circuit parameters for a parallel R, L circuit with constant parameters shown in Fig. 4. We select $V_m = 120\sqrt{2}$ V; $R = 1\,\Omega$; $L = 7$ mH; $f = 50$ Hz. We have solved the circuit analytically to compute current at the pcc. The voltage and current plots are shown in Fig. 5 left. Then, we have used only the values of the computed instantaneous voltage and current at the pcc to obtain the circuit parameters. Fig. 5 right, shows the results of the identification. One can see that the identification method returns near perfect results for $G = 1$ ($R = 1$) and $\Gamma = 142.9$ ($L = 0.007 \approx 1/142.9$) for all t. Table I gives the first five values used to compute the circuit parameters.

The significance of these results is major. To start, one can see that with very few points (only those necessary to compute the derivatives in (15) accurately) one can identify the circuit parameters of a linear circuit very efficiently and in a short time (under a millisecond for this case with a time step of 0.2 ms. We remark that no information on the original circuit topology is needed to apply the proposed identification method. The method allows for the identification of circuit parameters of a variety of circuit configurations given a set of voltage and current. This example sets the stage for the identification of nonlinear circuits from measurements of the instantaneous (discretized) current and voltage at the pcc.

B. Example 2: Parallel Circuit with Sinusoidal Excitation and non-Linear $R - L$ Elements

Fig. 6 shows a nonlinear circuit excited by a cosinusoidal source. The nonlinear elements vary according to the descriptions of Fig. 7. The resistor is switched on and off at the given times (unsymmetrical on purpose). The inductor saturates at $\phi_s = \pm 0.4$ Wb when the incremental inductance (the slope of the $\phi - i$ curve) changes from 7 mH to 1 mH. Three cases are presented as nonlinear examples: (a) when only the switch operates and the inductor remains constant at 7 mH; (b) when the switch is closed all the time and the inductor saturates; and (c) when both the switch operates and the inductor saturates. Fig. 8 shows the results for the three cases. The left-hand side plots, Figs. 8 a), c), and e), show the currents and voltages for the three cases. The right-hand side plots, Figs. 8 b), d), and f), show the results of the identification. One can see that the results are precise as the method has properly identified the circuit parameters from only the knowledge of current and voltage at the pcc. An outlier elimination algorithm has been used to remove spurious spikes caused by the numerical differentiation of sharp discrete functions. We conclude that the method put forward in this paper is capable of identifying the elements of nonlinear circuits even under the extremely distorted currents used in these examples.

C. Example 3: Parallel Circuit with Non-Sinusoidal Excitation and non-Linear $R - L$ Elements

The last example of this section is the identification of both the switching resistor and the saturating inductance when the excitation is non-sinusoidal. We take a 50 Hz excitation voltage with a large third harmonic given by:

$$v(t) = 120\sqrt{2}\cos\omega t + 40\sqrt{2}\cos 3\omega t$$

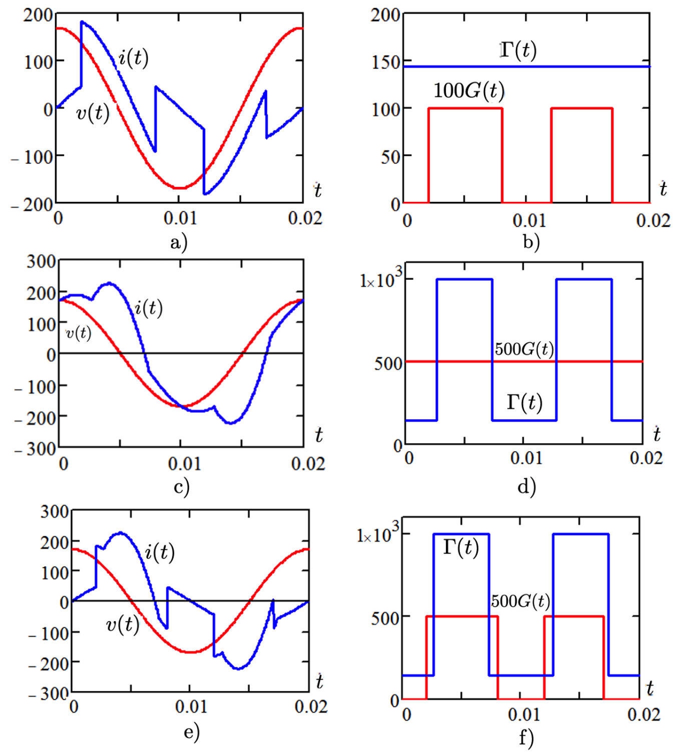

Figure 8. Simulations of nonlinear circuit of Fig. 6 and circuit parameter identification. (a) Voltage and current when the switch operates; (b) Identified Γ and G; (c) Voltage and current when the inductor saturates; (d) Identified Γ and G; (e) Voltage and current when the switch operates and the inductor saturates; (f) Identified Γ and G.

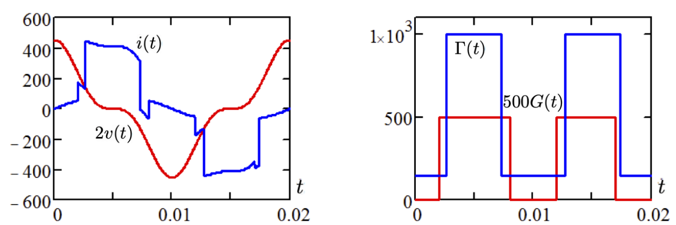

Figure 9. Simulations of nonlinear circuit of Fig. 6 with nonsinusoidal excitation and circuit parameter identification. left) Voltage and current; right) Identified Γ and G. Compare with Figs. 8(e) and 8(f).

Fig. 9 left presents this voltage and the corresponding current when both the switch operates and the inductor saturates. Fig. 9 right shows the results of the identification. As it can be seen, the identification is picture-perfect again even for this highly nonlinear circuit. This gives great confidence in the correctness of the method.

A large number of cases have been identified successfully, but the space in a paper is limited. The interested reader is directed to the following repository where the Matlab code for many cases has been posted in https://electrica.ual.es/spacor.

IV. Derivation of the Series Equivalent Circuit

In this section, the identification method for RL series circuits is presented. This requires the calculation of only two parameters R and L. We select the series circuit of Fig. 2 left (without C for now). To compute the series circuit, we now select a spacor that contains the current, its derivative, and voltage, for mathematical convenience as follows:

$$\boldsymbol{z} = i\boldsymbol{e}_1 + i'\boldsymbol{e}_2 + v\boldsymbol{e}_3 \tag{16}$$

Table I
FIRST FIVE VALUES OF THE VARIABLES IN (15)

t [ms]	v [V]	v' [V/s]	$\tilde{v}$ [V·s]	v^2 [V^2]	i [A]	i' [A/s]	G [Ω^{-1}]	Γ [H^{-1}]
0.0	0.0000	5331	-0.540	0.000	-77.170	5331	1.0	142.9
0.2	10.656	5231	-0.539	113.5	-66.362	5473	1.0	142.9
0.4	21.270	5289	-0.536	452.4	-55.292	5593	1.0	142.9
0.6	31.800	5237	-0.531	1011	-44.003	5691	1.0	142.9
0.8	42.204	5164	-0.523	1781	-32.541	5767	1.0	142.9

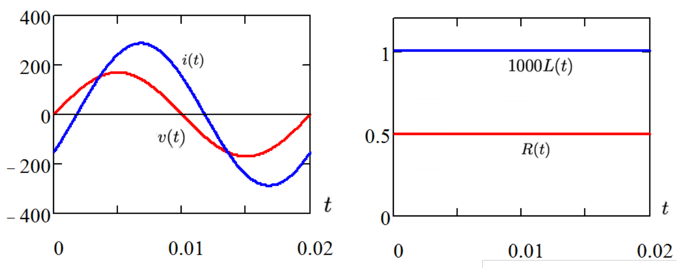

Figure 10. Time variation of parameters for the series RL case. left) voltage and current vs time at the pcc; right) identified resistance R and inductance L.

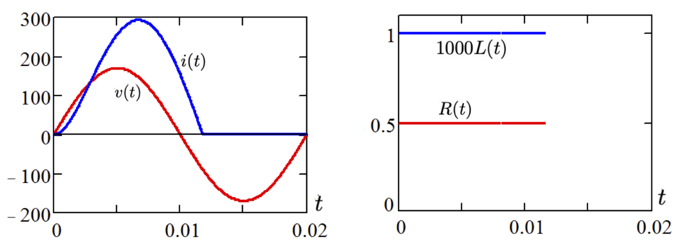

Figure 11. Simulations of a half-wave rectifier. left) Voltage and current; right) Identified R and L

Using a similar reasoning and following all steps from (7) to (14) of the parallel case, we arrive to:

$$R = \frac{v'i''' - i''v''}{i'i''' - i''^2} \qquad L = \frac{i'v'' - v'i''}{i'i''' - i''^2} \tag{17}$$

The supplemental material (at the end of the paper) shows the derivation step-by-step. This material will not be part of the paper but will be posted in the repository.

A. Example 4: Series Circuit with Sinusoidal Excitation and Linear R-L Elements

The first example to illustrate the series circuit parameter identification method is an RL circuit with constant parameters. We select $V_m = 120\sqrt{2}$ V; $R = 0.5\,\Omega$; $L = 1$ mH; $f = 50$ Hz The voltage and current plots are shown in Fig. 10 left). One can see that the identification method of this paper returns flawless results $R = 0.5\,\Omega$ and $L = 1$ mH for all t; see Fig. 10 right.

B. Example 5: Series Circuit with Sinusoidal Excitation and Non-Linear Circuits

The series model can be used for the identification of nonlinear circuits as well. Example 5 is a half-wave rectifier composed by a series of an ideal diode and a RL. The resistor is $0.5\,\Omega$, the inductor is $1\ mH$ and the excitation is the sinusoidal source of Example 4. This results in the voltage and current waveshapes given in Fig. 11 left. Using the series circuit identification process given by (16), we get the results illustrated in Fig. 11 right. As shown, the method perfectly identifies the original parameters until they disappear at time $t = 0.0118$ when the diode stops conducting after all the energy stored in the inductor has been returned to the source or consumed in the resistor.

V. IDENTIFICATION OF CIRCUITS WITH CAPACITANCE

The methods and examples presented so far identify only two passive elements R (or G) and L (or Γ). This is all that is needed for most cases since loads are predominantly inductive. Nevertheless, there are occasions when it may be necessary to find the capacitance independently from the inductance. We note that such cases are only meaningful when the excitation is non-sinusoidal since with sinusoidal excitation the energy stored/restored processes between an inductor and capacitor occur at unison (in the opposite direction). In other words, it is known that under sinusoidal excitation, inductors and capacitors compensate each other (partially or totally) and this is reflected in the current at the pcc. The identification of three-element circuits using GA becomes the simple matter of adding one more dimension to the spacors (planes become volumes) and follow the same process as in Section III.

A. Parallel Circuit with Three Elements

For the parallel case we construct a new spacor $\boldsymbol{y}$, as an extension of (6), defined as:

$$\boldsymbol{y} = v\boldsymbol{e}_1 + \tilde{v}\boldsymbol{e}_2 + v'\boldsymbol{e}_3 + i\boldsymbol{e}_4 \tag{18}$$

Voltage derivative v' has been selected because it is present in KCL (4) and we can combine it. Substituting i from (4) we get:

$$\boldsymbol{y} = v\underbrace{(\boldsymbol{e}_1 + G\boldsymbol{e}_4)}_{\boldsymbol{a}} + \tilde{v}\underbrace{(\boldsymbol{e}_2 + \Gamma\boldsymbol{e}_4)}_{\boldsymbol{b}} + v'\underbrace{(\boldsymbol{e}_3 + C\boldsymbol{e}_4)}_{\boldsymbol{c}} \tag{19}$$

The wedge product of vectors $\boldsymbol{a}\wedge\boldsymbol{b}\wedge\boldsymbol{c}$ gives the following volume (see Appendix A for detailed calculation of the trivectors $\boldsymbol{e}_{ijk}$):

$$\boldsymbol{K} = \boldsymbol{e}_{123} + C\boldsymbol{e}_{124} + G\boldsymbol{e}_{234} - \Gamma\boldsymbol{e}_{134} \tag{20}$$

The derivatives of (23) are:

$$\begin{aligned}
\boldsymbol{y}' &= v'\boldsymbol{e}_1 + v\boldsymbol{e}_2 + v''\boldsymbol{e}_3 + i'\boldsymbol{e}_4 \\
\boldsymbol{y}'' &= v''\boldsymbol{e}_1 + v'\boldsymbol{e}_2 + v'''\boldsymbol{e}_3 + i''\boldsymbol{e}_4 \\
\boldsymbol{y}''' &= v'''\boldsymbol{e}_1 + v''\boldsymbol{e}_2 + v''''\boldsymbol{e}_3 + i'''\boldsymbol{e}_4
\end{aligned} \tag{21}$$

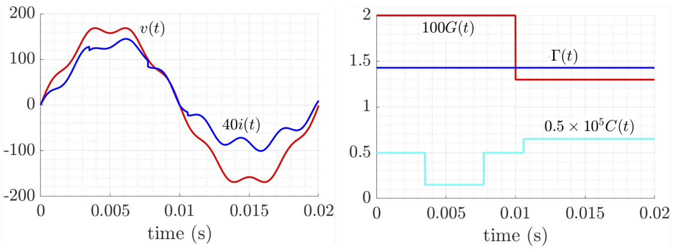

Figure 12. Three parameter identification method with a nonsinusoidal source. left) Voltage and current; right) Identified G, Γ and C.

The wedge product of spacors $\boldsymbol{y}'\wedge\boldsymbol{y}''\wedge\boldsymbol{y}'''$ gives the following expression for the osculating volume:

$$
\begin{aligned}
&\boldsymbol{K}_{osc} = \boldsymbol{y}'\wedge\boldsymbol{y}''\wedge\boldsymbol{y}''' = \\
&= \left[v''''\left(v'^2 - v''v\right) - v''\left(v'v''' - v''^2\right) + v'''\left(vv''' - v'v''\right)\right]\boldsymbol{e}_{123} \\
&+ \left[i'''\left(v'^2 - v''v\right) - v''\left(v'i'' - v''i'\right) + v'''\left(vi'' - v'i'\right)\right]\boldsymbol{e}_{124} \\
&+ \left[i'''\left(v'v''' - v''^2\right) - v''''\left(v'i'' - v''i'\right) + v'''\left(v''i'' - v'''i'\right)\right]\boldsymbol{e}_{134} \\
&+ \left[i'''\left(vv''' - v'v''\right) - v''''\left(vi'' - v'i'\right) + v''\left(v''i'' - v'''i'\right)\right]\boldsymbol{e}_{234}
\end{aligned} \tag{22}
$$

Comparing term-to-term of (19) with (21) we get the expressions to compute the circuit elements as follows:

$$
\begin{aligned}
G &= \frac{i'''\left(vv''' - v'v''\right) - v''''\left(vi'' - v'i'\right) + v''\left(v''i'' - v'''i'\right)}{v''''\left(v'^2 - v''v\right) - v''\left(v'v''' - v''^2\right) + v'''\left(vv''' - v'v''\right)} \\
\Gamma &= -\frac{i'''\left(v'v''' - v''^2\right) - v''''\left(v'i'' - v''i'\right) + v'''\left(v''i'' - v'''i'\right)}{v''''\left(v'^2 - v''v\right) - v''\left(v'v''' - v''^2\right) + v'''\left(vv''' - v'v''\right)} \\
C &= \frac{i'''\left(v'^2 - v''v\right) - v''\left(v'i'' - v''i'\right) + v'''\left(vi'' - v'i'\right)}{v''''\left(v'^2 - v''v\right) - v''\left(v'v''' - v''^2\right) + v'''\left(vv''' - v'v''\right)}
\end{aligned} \tag{23}
$$

Clearly, the need for computation of an extra parameter C adds complexity to the obtained formulas. However, the result is an impeccable identification of parameters as shown below. Next is an example of circuit parameter identification for three parallel elements G, Γ, and C as in Fig. 2 right fed from a nonsinusoidal voltage 50 Hz source that has the following function (fundamental plus seventh harmonic):

$$v(t) = 120\sqrt{2}\sin\omega t + 12\sin 7\omega t$$

We select a linear (constant) inductor of 0.7 H, a resisitor that changes from $50\,\Omega$ to $77\,\Omega$ at 10 ms, and a capacitor that takes the following values:

$$
C(t) = \begin{cases}
10\ \mu\text{F} & 0 \le t \le 3.5\ \text{ms} \\
3\ \mu\text{F} & 3.5 < t \le 7.72\ \text{ms} \\
10\ \mu\text{F} & 7.72 < t \le 10.58\ \text{ms} \\
13\ \mu\text{F} & 10.58 < t < 20\ \text{ms}
\end{cases}
$$

Fig. 12 left shows the current and voltage and Fig. 12 right shows the identified circuit elements obtained with (22). As before, one can see that that identification is accurate (after the outlier spikes have been filtered out).

We remark that the three-parameter identification method only works when the excitation is non-sinusoidal. As mentioned above, under sinusoidal conditions, the reactive power of inductors and capacitors cancel (partially or fully) each other. Thus, (14) should be used because the denominator in (22) is always zero. To avoid the singularity for sinusoidal excitation a very small voltage harmonic can be added. The problem is solved even if a 10^{-12} of any voltage harmonic is added. In practice, this is not a problem because real voltages always have some distortion (even if very small).

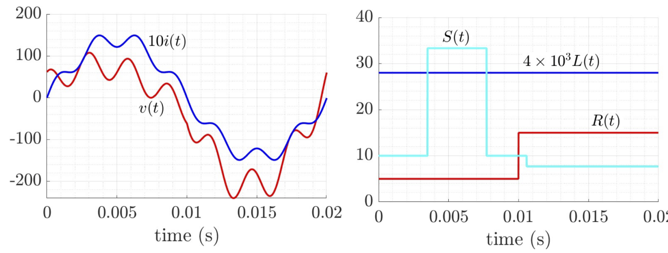

Figure 13. Three parameter identification method with a nonsinusoidal source for a series circuit. left) Voltage and current; right) Identified R, L and S

B. Series Circuit with Three Elements

For the series circuit we select the following spacor:

$$\boldsymbol{z} = i\boldsymbol{e}_1 + \tilde{\imath}\boldsymbol{e}_2 + i'\boldsymbol{e}_3 + v\boldsymbol{e}_4 \tag{24}$$

Following the same procedure, we get the formulae for the calculation of the circuit parameters:

$$
\begin{aligned}
R &= \frac{v'''\left(ii''' - i'i''\right) - i''''\left(iv'' - i'v'\right) + i''\left(i''v'' - i'''v'\right)}{i''''\left(i'^2 - i''i\right) - i''\left(i'i''' - i''^2\right) + i'''\left(ii''' - i'i''\right)} \\
S &= -\frac{v'''\left(i'i''' - i''^2\right) - i''''\left(i'v'' - i''v'\right) + i'''\left(i''v'' - i'''v'\right)}{i''''\left(i'^2 - i''i\right) - i''\left(i'i''' - i''^2\right) + i'''\left(ii''' - i'i''\right)} \\
L &= \frac{v'''\left(i'^2 - i''i\right) - i''\left(i'v'' - i''v'\right) + i'''\left(iv'' - i'v'\right)}{i''''\left(i'^2 - i''i\right) - i''\left(i'i''' - i''^2\right) + i'''\left(ii''' - i'i''\right)}
\end{aligned} \tag{25}
$$

One can see that (24) and (22) have identical shape and can be obtained from each other by switching v by i and vice versa. This is can be foreseen when comparing (17) and (23).

The example for this section consists of a series RLC circuit with varying resistor and capacitor and a constant inductor. The following nonsinusoidal (50 Hz) current source is used to excite the circuit:

$$i(t) = 10\sqrt{2}\sin\omega t + 2\sin 7\omega t$$

We select a linear (constant) inductor of 7 mH, a resistor that changes from $5\,\Omega$ to $15\,\Omega$ at 10 ms, and the same capacitor from the previous example. The results are illustrated in Fig. 13. The voltage and current at the pcc are shown in Fig. 13 left and the variation of the identified circuit parameters in Fig. 13 right). Once again, one can observe a perfect identification (after outliers have been removed).

VI. Power and Energy

Once that the circuit parameters have been obtained, the power and energy consumed and stored/restored can be computed from first electromagnetic principles (Maxwell Equations). There is no need to rely on any of the power definitions proposed in the standard, some of which do not have physical existence even for simple cases. With our method, there are no physical interpretation problems because we compute (rather than define) power and energy from the most fundamental concepts of the Poynting Vector Theorem as applied to circuit theory (under the quasistatic condition).

A. Instantaneous Power Consumed and Energy Stored

According to Joule's law the instantaneous power consumed (p_{cons}) in an electric circuit is computed from [1]:

$$p_{\text{cons}} = v_R i_R = R i_R^2 = G {v_R}^2 \tag{26}$$

The instantaneous energy stored in an inductor or capacitor (w_{stor} in electromagnetic fields) can be obtained from Maxwell [2] as:

$$w_{\text{stor}(L)} = \frac{1}{2}\iint_V \bar{H}\cdot d\bar{B} \quad w_{\text{stor}(C)} = \frac{1}{2}\iint_V \bar{E}\cdot d\bar{D} \quad (27)$$

where H is the magnetic field strength, B is the magnetic flux density, E is the electric field strength, and D is the electric flux density. For quasistatic fields in isotropic and homogenous media but allowing for nonlinear behavior (saturation and hysteresis), (26) can be written as:

$$w_{\text{stor}(L)} = \int i d\phi \qquad w_{\text{stor}(C)} = \int v dq \quad (28)$$

where i and ϕ are the current and flux in the inductor, v and q are the voltage and charge in the capacitor. Ampere's law is used to relate H with i and surface integral to relate B with ϕ. Gauss's law is used to get q from D and the line integral of E yields v. The effective inductance and capacitance are related to the energy stored through the following familiar formulae:

$$w_{\text{stor}(L)} = \frac{1}{2}L_{\text{eff}}i^2 \qquad w_{\text{stor}(C)} = \frac{1}{2}C_{\text{eff}}v^2 \quad (29)$$

In this paper, equation (27) is used to compute the energy stored because we identify the circuit elements point-by-point. The integral to compute the area (representing the energy stored in Fig. 3) is obtained following the variations of the incremental inductance. The effective instantaneous inductance (L_{eff} and capacitance C_{eff}) can be computed from (28) once that (27) has been evaluated. The apparent inductance L_{app} and capacitance C_{app} can be computed in straightforward manner from an operating point (t_0) as:

$$L_{\text{app}} = \frac{\phi(t_0)}{i(t_0)} = \frac{\int_0^{t_0} vdt}{i(t_0)}; C_{\text{app}} = \frac{q(t_0)}{v(t_0)} = \frac{\int_0^{t_0} idt}{v(t_0)} \quad (30)$$

To compute the instantaneous (reactive) power in inductors and capacitors we apply the chain rule to (27) to have the expression as a function of time only. Thus (27) becomes:

$$w_{\text{stor}(L)} = \int v_L i_L dt \qquad w_{\text{stor}(C)} = \int v_C i_C dt \quad (31)$$

Taking the derivative with time, we get the instantaneous (reactive) powers (p_{reac}):

$$\begin{aligned} p_{\text{reac}(L)} &= \frac{d}{dt}w_{\text{stor}(L)} = v_L i_L \\ p_{\text{reac}(C)} &= \frac{d}{dt}w_{\text{stor}(C)} = v_C i_C \end{aligned} \quad (32)$$

Equations (31) apply to the series and parallel equivalent circuits and are in perfect agreement with circuit theory (power is the product of current through the element multiplied by the voltage across the element). For the parallel circuit the voltage is the one measured at the pcc $(v = v_L = v_C)$ and the element currents are computed from the identified Γ and C as:

$$i_L = \int \Gamma v dt \qquad i_C = C\frac{dv}{dt} \quad (33)$$

The instantaneous reactive power in the parallel circuit is calculated from

$$p_{\text{reac}} = p_{\text{reac}(L)} + p_{\text{reac}(C)} = v i_L + v i_C \quad (34)$$

$$p_{\text{reac}} = v\int \Gamma v dt + vCv' \quad (35)$$

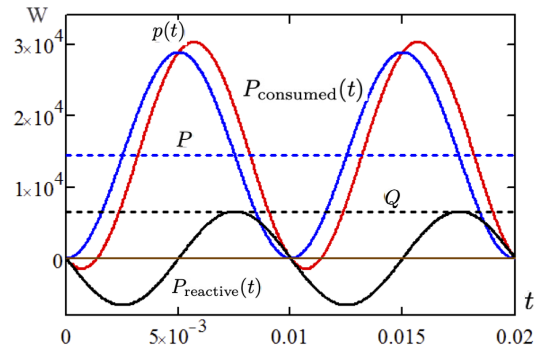

Figure 14. Power quantities for the parallel circuit of Example 1.

Note that for linear circuits (Γ and C are constant) with sinusoidal excitation, $\tilde{v}$ and v' are in the exact opposite directions (one of them is negative when the other is positive) and partial or total cancellation occurs. When the excitation is nonsinusoidal $p_{\text{reac}(L)}$ and $p_{\text{reac}(C)}$ in (33) do not subtract from each other at every instant. For the series circuit, the current is the one measured at the pcc $(i = i_L = ic)$ and the element voltages are computed from the identified L and S as:

$$v_L = L\frac{di}{dt} \qquad v_C = \int Sidt \quad (36)$$

The instantaneous reactive power in the series circuit is calculated from

$$p_{\text{reac}} = p_{\text{reac}(L)} + p_{\text{reac}(L)} = v_L i + v_C i \quad (37)$$

$$p_{\text{reac}} = iLi' + i\int Sidt \quad (38)$$

As before, for linear circuits (L and S are constant) with sinusoidal excitation $\tilde{\imath}$ and i' are in the exact opposite directions (one of them is negative when the other is positive). The equations of this section are completely general and are applicable to any linear or nonlinear single-phase circuit with sinusoidal or nonsinusoidal excitation. Note that all these quantities are given in physical quantities, i.e., Watts or Joules; even the instantaneous reactive powers are in watts (vars do not exist in time domain). One can verify that the following equalities are always fulfilled:

$$p = vi = p_{\text{cons}} + p_{\text{reac}} \quad (39)$$

$$P = \bar{p} = \tfrac{1}{T}\int_0^T pdt = \tfrac{1}{T}\int_0^T vidt = \tfrac{1}{T}\int_0^T Ri_R^2 dt = \tfrac{1}{T}\int_0^T Gv_R^2 dt \quad (40)$$

$$\tfrac{1}{T}\int_0^T p_{\text{reac}(L)}dt = 0; \tfrac{1}{T}\int_0^T p_{\text{reac(C)}}dt = 0; \tfrac{1}{T}\int_0^T p_{\text{reac}}dt = 0 \quad (41)$$

$$Q = \max(p_{\text{reac}}) \quad (42)$$

where P and Q are the traditional active and reactive powers. For linear circuits, P and Q in (39) and (41) match the traditional computation of active and reactive powers. The examples below show physically consistent results for all linear and non-linear cases tested. For instance, the balance of power equation (38) is always fulfilled even when it is not explicitly enforced in the calculation of powers.

B. Examples and Comparison with other Power Theories

Fig. 14 shows the result of the power computed for the linear circuit identified in Example 1 (Fig. 4). One can see that there is no need to use any definition of power to compute the

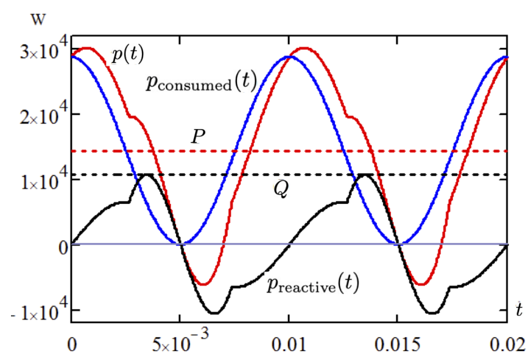

Figure 15. Power quantities for the parallel circuit of Example 2 with linear resistor and saturating inductor.

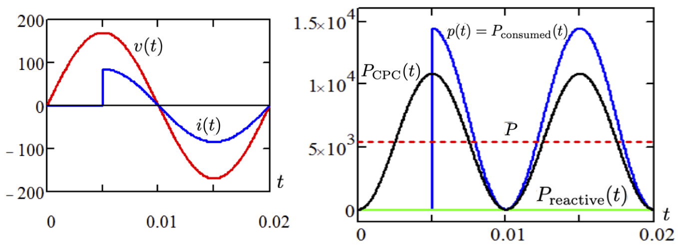

Figure 16. Power quantities for the example of [34].

physical results. For this linear case, P and Q of (39) and (41) coincide with the Steinmetz formulas [6]:

$$P = V_{\text{rms}} I_{\text{rms}} \cos\phi = R I_{R_{\text{rms}}}^2 = 14.4 \text{ kW} \tag{43}$$

$$Q = V_{\text{rms}} I_{\text{rms}} \sin\phi = -\omega L I_{L_{\text{rms}}}^2 = -6.55\text{kvar} \tag{44}$$

Now consider the case of Example 2, which consists of a linear resistor and a saturating inductor with sinusoidal excitation. Fig. 15 shows the results. One can see that the instantaneous power consumed and reactive powers fulfill with (39) and (40), which gives assurance on the correctness of the method. In this case, P is the same as in (42), but Q is now:

$$Q = -\max(p_{\text{reac}}) = -\max\left(\frac{d}{dt} w_{\text{stor}}\right) = -10.68 \text{ kW} \tag{45}$$

Q is expressed in kW to properly represent the power corresponding to the energy stored. The negative sign is used because of the convention that inductive power is negative. The fundamental reactive power from the IEEE Standard (Section 3.1.2.6) [9] is:

$$Q_1 = V_1 I_1 \sin\theta_1 = (120)(112.5)(-0.657) = -12.53\text{kvar} \tag{46}$$

As shown in [35] this is the "compensable" power, but it is not related to the time derivative of the energy stored. The last example has been used in [34] to discredit many of the available reactive power definitions (including those in the IEEE Standard). The circuit consists of a sinusoidal (50 Hz) voltage source feeding a $2\,\Omega$ resistor that is switched on at 5 ms (and remains connected to the end of the period). Fig. 16 left shows the voltage and current and Fig. 16 right shows the power consumed and reactive power computed from (25) and (31) after the parameters have been correctly identified (series and parallel circuits yield the same results). A Fourier analysis of the current yields that there is a fundamental component of $I_1 =$ 65.057 A at an angle of $\phi_1 = -11.98$ degrees. Most available definitions of Q compute a non-physical reactive power. In particular the standard [9] gives a fundamental reactive power of $Q_1 = -1.146$ kvar. We remark that the circuit has no elements capable of storing energy! Our method properly computes $p_{\text{reac}}(\mathrm{t}) \equiv 0$ and therefore, $Q = 0$ as it should be. More examples are given in [36]. Other popular power theories, such as Czarnecki's Current Physical Components (CPC) [37] and Akagi's instantaneous $p-q$ powers [38] produce non-physical active and reactive powers. The problem with CPC starts with the instantaneous active current. i_{active} in [37] is "defined" using Fryze's conductance multiplied by the instantaneous voltage as:

$$i_{\text{active}} = \frac{P}{V_{rms}^2} v = G_{\text{Fryze}} v \tag{47}$$

G_{Fryze} is an average conductance and not the actual timevarying conductance (as computed in this paper). Fig. 16 right shows the active power computed from i_{active} of [37] labeled $\mathrm{P\_CPC(t)}$. One can see that this "active power" is very different from the actual instantaneous power consumed in the resistor (although it has the same average). A nonphysical reactive power is also computed; see more details in [36]. Akagi's $p-q$ instantaneous powers, although very useful for the design of compensators, fail to provide physical meaning to powers in very simple circuits; see [39].

We conclude that neither Q_1 from the standard [9], the CPC from [37], or $p-q$ from [38] physically represent active power as the power consumed (according to Joule) or the reactive power as the time derivative of the energy stored (according to Maxwell). Our $p_{\text{cons}}(t)$ and $p_{\text{reac}}(t)$ comply with all electromagnetic principles because they are computed from them. More examples have been posted in the repository for the reader to verify the correctness of the method in: htttps://electrica.ual.es/spacor.

VII. Conclusions

The paper has presented a novel method for the identification of circuit elements from measurements of the instantaneous voltage and current at the point of common coupling. Geometric algebra and differential geometry have been conveniently used because of their unique features for handling vectors and constructing planes and volumes that represent and model electrical parameters as geometric objects. The results have shown that the method is accurate and robust for the identification of parameters under severe nonlinear conditions. Once the circuit elements are computed, the power and energy consumed and stored are obtained from first electromagnetic principles. Therefore, the obtained quantities have no physical interpretation issues and can be conveniently employed for a variety of engineering problems such as current compensation, voltage stability, and load identification, to mention a few.

VIII. Future Applications

The methods proposed in this paper have applications beyond electric circuit parameter identification for power and energy computations. We foresee that, in the short-term, the method will be used for equipment condition monitoring, voltage stability analysis and control of microgrids, and calculation of equivalents for electromagnetic transient simulations. Moreover, the method will find applications beyond electric power engineering. For example, any system that can be made analog

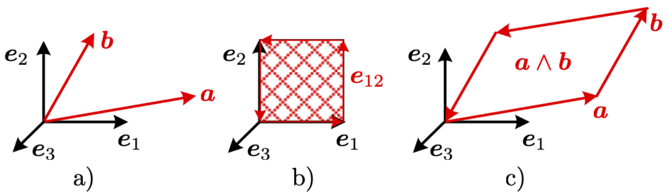

Figure A1. Illustration of a) orthonormal vector basis and vectors, b) unit bivector, and c) wedge product of vectors resulting in a bivector (plane).

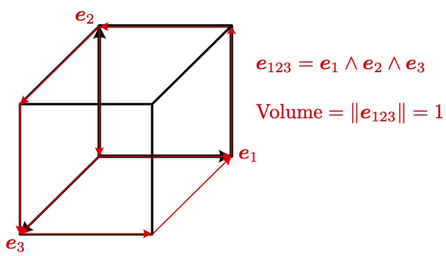

Figure A2. Illustration of a trivector or volume element.

to an electric circuit is likely to benefit from the methods of this paper. Mechanical (described by mass, spring, damping) and thermal or acoustic systems (represented by electrical equivalent circuits) would be excellent candidates. The derivation of the method for three-phase balanced and unbalanced systems will be presented in a forthcoming paper. The implementation of the method in a real life application will find challenges with the calculation of high-order derivatives. It is known that the evaluation of numerical derivatives is significantly affected by noise and abrupt changes in the signals. The following signal processing techniques will be explored for field implementation: signal filtering, high-order smooth differentiation, and outlier elimination.

APPENDIX A - BASIC CONCEPTS OF GA

In this section we briefly describe the basic concepts of geometric algebra necessary to understand the theory of the identification method of Section II. There are several advanced books for GA [21], [24], [30], [40], mainly devoted to Electromagnetism and general Physics. Yet to come is a basic book on GA suitable for the electrical or power engineer to describe the concepts used in this paper. At the moment (2021), online videos seem to be an alternative and highly recommended educational tool for this subject. We suggest the interested reader to follow these links:

1) https://www.youtube.com/watch?v=60z_hpEAtD8
2) https://www.youtube.com/watch?v=PNlgMPzj-7Q

Let us start with the classical definition of an orthonormal vector basis in 3D $(\boldsymbol{e}_1, \boldsymbol{e}_2, \boldsymbol{e}_3)$ as shown in Fig. A1. We use the postulates of exterior algebra to introduce a bilinear operation (wedge or exterior product) among vectors in an axiomatically way

$$\boldsymbol{a} \wedge \boldsymbol{a} = 0 \tag{A.1}$$

The wedge product of a vector with itself is zero. The wedge product is an associative, distributive, and anti-commutative operation. This is expressed mathematically as:

$$\begin{aligned} (\boldsymbol{a} \wedge \boldsymbol{b}) \wedge \boldsymbol{c} &= \boldsymbol{a} \wedge (\boldsymbol{b} \wedge \boldsymbol{c}) \\ \boldsymbol{a} \wedge (\boldsymbol{b} + \boldsymbol{c}) &= \boldsymbol{a} \wedge \boldsymbol{b} + \boldsymbol{a} \wedge \boldsymbol{c} \\ \boldsymbol{a} \wedge \boldsymbol{b} &= -\boldsymbol{b} \wedge \boldsymbol{a} \end{aligned} \tag{A.2}$$

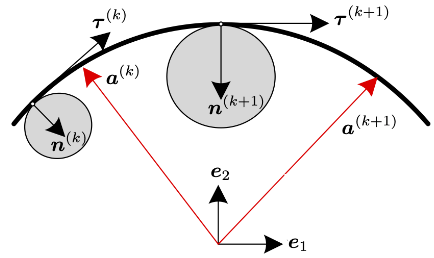

Figure B1. Illustration of several osculating circles for different time instants k and $k+1$ in a curve described by a time variant vector $\boldsymbol{a}$. $\boldsymbol{\tau}$ is the tangent vector and $\boldsymbol{n}$ the normal vector.

Based on the above definitions, orthogonal vectors have very interesting (and useful properties) in geometrical algebra:

$$\begin{aligned} &\boldsymbol{e}_1 \wedge \boldsymbol{e}_1 = 0 \\ &\boldsymbol{e}_{12} = \boldsymbol{e}_1 \wedge \boldsymbol{e}_2 = -\boldsymbol{e}_2 \wedge \boldsymbol{e}_1 = -\boldsymbol{e}_{21} \\ &\boldsymbol{e}_1 \wedge \boldsymbol{e}_2 \wedge \boldsymbol{e}_3 = \boldsymbol{e}_{123} \end{aligned} \tag{A.3}$$

The wedge product is a measure of similarity between vectors, but it is also a mechanism to build new high-dimensional objects from low-dimensional ones. Fig. A2 depicts the trivector $\boldsymbol{e}_{123}$. As one can see, it describes a volume. For simplicity, take two vectors $\boldsymbol{a}$ and $\boldsymbol{b}$ defined as:

$$\boldsymbol{a} = a_1 \boldsymbol{e}_1 + a_2 \boldsymbol{e}_2 \tag{A.4}$$

$$\boldsymbol{b} = b_1 \boldsymbol{e}_1 + b_2 \boldsymbol{e}_2 \tag{A.5}$$

where: $a_1, a_2, b_1, b_2 \in \mathbb{R}$, are the coordinates (possibly time varying). Following the rules in (A.3), a new geometric object called a bivector is defined by the wedge product of $\boldsymbol{a}$ and $\boldsymbol{b}$ as follows (similar to the cross product of traditional vector algebra):

$$\boldsymbol{a} \wedge \boldsymbol{b} = (a_1 b_2 - a_2 b_1)\, \boldsymbol{e}_1 \wedge \boldsymbol{e}_2 \tag{A.6}$$

The wedge product of the unitary vectors $\boldsymbol{e}_1 \wedge \boldsymbol{e}_2$ is commonly represented as $\boldsymbol{e}_{12}$ which represents an oriented plane; see Fig. A1. Its magnitude is the area of the parallelogram. We note that

$$e_{12} = e_1 \wedge e_2 = -e_2 \wedge e_1 = -e_{21} \tag{A.7}$$

$\boldsymbol{e}_{12}$ and $\boldsymbol{e}_{21}$ are bivectors with the same magnitude, but oriented in opposite direction. For the particular case of 3D, there exist a unique normal vector to the bivector $\boldsymbol{e}_{12}$. In this case, vector $\boldsymbol{e}_3$. In GA terms, $\boldsymbol{e}_3$ is the dual of $\boldsymbol{e}_{12}$. Note that this only happens in 3D, but not in any other dimension. This is the reason that the traditional cross product of vectors is only uniquely defined in 3D but does not work in higher dimensions. It is clear then from Fig. A1 that vectors $\boldsymbol{a}$ and $\boldsymbol{b}$ define a plane (which area is given by $\boldsymbol{a} \wedge \boldsymbol{b}$) and from Fig. A2 that vectors $\boldsymbol{a}, \boldsymbol{b}$ and $\boldsymbol{c}$ define a volume.

APPENDIX B - BASIC CONCEPTS OF DIFFERENTIAL GEOMETRY

Another necessary concept for the identification method of this paper is the osculating plane/circle (in 2D) or the osculating volume (in 3D), and so on as more dimensions are used.

To compute an osculating plane of a curve, we use the basic principles of differential geometry in particular the Frenet-Serret Frame (FSF) [31]. Just like in traditional calculus where we compute the tangent of a curve at a given point by taking the derivative, one can take the derivative of a vector to obtain the tangent vector. Fig. B1 shows a drawing of the time variation trajectory of vector $\boldsymbol{a}$. The figure also contains two osculating planes for two different time instants. The osculating plane is obtained by the wedge product of the first and second derivatives of the vector:

$$\boldsymbol{K}_{\text{osc}} = \boldsymbol{a}' \wedge \boldsymbol{a}'' \tag{A.8}$$

For the 3D case, the osculating volume is obtained from the first, second, and third derivatives:

$$\boldsymbol{K}_{\text{osc}} = \boldsymbol{a}' \wedge \boldsymbol{a}'' \wedge \boldsymbol{a}'' \tag{A.9}$$

ACKNOWLEDGMENT

The authors would like to thank Dr. Dimitri Jeltsema from Han University for interesting discussions on the mathematical and physical concepts of electric power and geometric algebra.

REFERENCES

[1] J. P. Joule, "On the heat evolved by metallic conductors of electricity, and in the cells of a battery during electrolysis," *The London, Edinburgh, and Dublin Philosophical Magazine and Journal of Science*, vol. 19, no. 124, pp. 260–277, 1841.

[2] J. C. Maxwell, *A treatise on electricity and magnetism*. Clarendon press, 1873, vol. 1.

[3] J. H. Poynting, "On the transfer of energy in the electromagnetic field," *Philosophical Transactions of the Royal Society of London*, no. 175, pp. 343–361, 1884.

[4] A. E. Kennelly, "Impedance," *Transactions of the American Institute of Electrical Engineers*, vol. 10, pp. 172–232, 1893.

[5] C. P. Steinmetz, "Complex quantities and their use in electrical engineering," in *Proceedings of the International Electrical Congress*, 1893, pp. 33–74.

[6] C. P. Steinmetz, *Theory and calculation of alternating current phenomena*. McGraw-Hill Book Company, Incorporated, 1916, vol. 4.

[7] S. J. Committee *et al.*, "Power factor in polyphase circuits," *Transactions of the American Institute of Electrical Engineers*, vol. 39, no. 2, pp. 1449–1450, 1920.

[8] A. E. Knowlton, "Reactive power concepts in need of clarification," *Electrical Engineering*, vol. 52, no. 4, pp. 259–262, 1933.

[9] R. Langella and A. Testa, "IEEE standard definitions for the measurement of electric power quantities under sinusoidal, nonsinusoidal, balanced, or unbalanced conditions," *Revision of IEEE Std*, pp. 1459–2000, 2010.

[10] M. Malengret and C. T. Gaunt, "Active currents, power factor, and apparent power for practical power delivery systems," *IEEE Access*, vol. 8, pp. 133 095–133 113, 2020.

[11] L. S. Czarnecki, "Why the power theory has a limited contribution to studies on the supply and loading quality?" in *2018 18th International Conference on Harmonics and Quality of Power (ICHQP)*. IEEE, 2018, pp. 1–6.

[12] L. S. Czarnecki and P. M. Haley, "Power properties of four-wire systems at nonsinusoidal supply voltage," *IEEE Trans. Power Del.*, vol. 31, no. 2, pp. 513–521, 2015.

[13] L. S. Czarnecki and M. Almousa, "Adaptive balancing of three-phase loads at four-wire supply with reactive compensators and nonsinusoidal voltage," in *2020 IEEE Texas Power and Energy Conference (TPEC)*. IEEE, 2020, pp. 1–6.

[14] C. Burgos-Mellado, R. Cárdenas, D. Saez, A. Costabeber, and M. Sumner, "A control algorithm based on the conservative power theory for cooperative sharing of imbalances in four-wire systems," *IEEE Trans. Power Electron.*, vol. 34, no. 6, pp. 5325–5339, 2018.

[18] A. Petroianu, *Bridging Circuits and Fields: Foundational Questions in Power Theory*. CRC Press, Taylor & Francis Group, 2021. [Online]. Available: https://books.google.es/books?id=rjTevgEACAAJ

[15] W. Shepherd and P. Zand, *Energy flow and power factor in nonsinusoidal circuits*. Cambridge University Press, 1979.

[16] H. Akagi, E. H. Watanabe, and M. Aredes, *Instantaneous power theory and applications to power conditioning*. John Wiley & Sons, 2017.

[17] A. E. Emanuel, *Power definitions and the physical mechanism of power flow*. John Wiley & Sons, 2011, vol. 22.

[19] P. Tenti, P. Mattavelli *et al.*, "A time-domain approach to power term definitions under non-sinusoidal conditions," in *Sixth international workshop on power definitions and measurements under non-sinusoidal conditions*, no. 35, 2003, p. 34.

[20] T. Hong and F. De León, "Lissajous curve methods for the identification of nonlinear circuits: Calculation of a physical consistent reactive power," *IEEE Trans. Circuits Syst. I*, vol. 62, no. 12, pp. 2874–2885, 2015.

[21] D. Hestenes and G. Sobczyk, *Clifford algebra to geometric calculus: a unified language for mathematics and physics*. Springer Science & Business Media, 2012, vol. 5.

[22] F. G. Montoya, R. Baños, A. Alcayde, F. M. Arrabal-Campos, and J. Roldán-Pérez, "Vector geometric algebra in power systems: An updated formulation of apparent power under non-sinusoidal conditions," *Mathematics*, vol. 9, no. 11, p. 1295, 2021.

[23] D. Hestenes, "Spacetime physics with geometric algebra," *American Journal of Physics*, vol. 71, no. 7, pp. 691–714, 2003.

[24] B. Jancewicz, *Multivectors and Clifford algebra in electrodynamics*. World Scientific, 1989.

[25] D. Hildenbrand, J. Zamora, and E. Bayro-Corrochano, "Inverse kinematics computation in computer graphics and robotics using conformal geometric algebra," *Advances in applied Clifford algebras*, vol. 18, no. 3-4, pp. 699–713, 2008.

[26] F. G. Montoya, R. Baños, A. Alcayde, F. M. Arrabal-Campos, and J. Roldán Pérez, "Geometric algebra framework applied to symmetrical balanced three-phase systems for sinusoidal and non-sinusoidal voltage supply," *Mathematics*, vol. 9, no. 11, p. 1259, 2021.

[27] F. G. Montoya, A. Alcayde, F. M. Arrabal-Campos, and R. Banos, "How to overcome the limitations of pq theory: Geometric algebra power theory to the rescue," in *2020 IEEE PES Innovative Smart Grid Technologies Europe (ISGT-Europe)*. IEEE, 2020, pp. 339–343.

[28] H. A. Tilmans, "Equivalent circuit representation of electromechanical transducers: I. lumped-parameter systems," *Journal of Micromechanics and Microengineering*, vol. 6, no. 1, p. 157, 1996.

[29] "The authoritative dictionary of ieee standards terms, seventh edition," *IEEE Std 100-2000*, pp. 1–1362, 2000.

[30] A. Macdonald, *Linear and geometric algebra*. Alan Macdonald, 2010.

[31] J. Snygg, *A new approach to differential geometry using Clifford's geometric algebra*. Springer Science & Business Media, 2011.

[32] J. F. Kaiser, "On a simple algorithm to calculate the'energy'of a signal," in *International conference on acoustics, speech, and signal processing*. IEEE, 1990, pp. 381–384.

[33] I. Kamwa, A. K. Pradhan, and G. Joós, "Robust detection and analysis of power system oscillations using the teager-kaiser energy operator," *IEEE Transactions on Power Systems*, vol. 26, no. 1, pp. 323–333, 2010.

[34] F. De Leon and J. Cohen, "Discussion of 'An evaluation of some alternative methods of power resolution in a large industrial plant'," *IEEE Trans. Power Del.*, vol. 18, no. 2, pp. 658–659, 2003.

[35] F. De Leon and J. Cohen, "A practical approach to power factor definitions: transmission losses, reactive power compensation, and machine utilization," in *2006 IEEE Power Engineering Society General Meeting*. IEEE, 2006, pp. 7–pp.

[36] F. De Leon and J. Cohen, "Discussion of 'Instantaneous reactive power pq theory and power properties of three-phase systems'," *IEEE Trans. Power Del.*, vol. 23, no. 3, pp. 1693–1694, 2008.

[37] L. S. Czarnecki, "Currents' physical components (cpc) concept: A fundamental of power theory," in *2008 International School on Nonsinusoidal Currents and Compensation*. IEEE, 2008, pp. 1–11.

[38] H. Akagi, Y. Kanazawa, K. Fugita, and A. Nabe, "Generalized theory of instantaneous reactive power and its application," electrical engg," 1983.

[39] F. De Leon and J. Cohen, "Discussion of 'Generalized theory of instantaneous reactive quantity for multiphase power system'," *IEEE Trans. Power Del.*, vol. 21, no. 1, pp. 540–541, 2005.

[40] J. W. Arthur, *Understanding geometric algebra for electromagnetic theory*. John Wiley & Sons, 2011, vol. 38.